Journal of Applied Polymer Science

Diffusion Measurements of Isopentane, 1-Hexene, Cyclohexane in Polyethylene Particles by the Intelligent Gravimetric Analyzer

Meijuan Chen, Jingdai Wang, Binbo Jiang, Yongrong Yang
State Key Laboratory of Chemical Engineering, Department of Chemical and Biochemical Engineering, Zhejiang University, Hangzhou 310027, People's Republic of China

Correspondence to: J. Wang (E-mail: wangjd@zju.edu.cn)

ABSTRACT: The diffusion coefficients of isopentane (i-C_5H_{12}), 1-hexene (C_6H_{12}), cyclohexane (C_6H_{14}) in polyethylene particles were measured by a highly sensible microbalance—intelligent gravimetric analyzer, using the desorption method with N_2 as a bypassing gas. Both the effective diffusion coefficients (D_{eff}) and dilute diffusion coefficients ($D_{eff}^{\sim}$) were measured simultaneously. It was found that $D_{eff}^{\sim}$ was about one magnitude smaller than D_{eff} and the logarithmic form of $D_{eff}^{\sim}$ was linear with that of D_{eff}. In addition, the effects of particle size and distribution, polymer properties (e.g., the crystallinity and melt index), and operating conditions (e.g., temperature and pressure) on D_{eff} were systematically investigated. The results showed that D_{eff} increased linearly with the increase of the square of particle size. The diffusion behaviors of hydrocarbons in polyethylene are of great importance in the polymerization and purging processes. © 2010 Wiley Periodicals, Inc. J. Appl. Polym. Sci. 000: 000–000, 2012

KEYWORDS: hydrocarbon; polyethylene (PE); particles size and distribution; diffusion; dilute diffusion coefficients

Received 14 October 2011; accepted 24 April 2012; published online
DOI: 10.1002/app.37948

INTRODUCTION

Polyolefin is one of the most widely applied polymer families for its abundant availability, low cost, and various application fields. The key procedure of producing polyolefin is the polymerization reaction, during which the polymer particles are formed in the reactor with catalyst, monomer (ethylene, propylene), comonomer (1-hexene), and condensing agents (isopentane) or solvents (cyclohexane). After polymerization, the polyolefin particles discharged from the reactor inevitably contain these unreacted hydrocarbons, which must be purged to comply with environmental regulations and ensure the safety of our products. The purging process is called devolatilization.[1] Recovering and recycling these unreacted hydrocarbons back to the reactor also reduces the production cost. Therefore, the diffusion behaviors of hydrocarbons in polyolefin are of great importance in the polymerization and devolatilization, which have been studied extensively.

However, it is still difficult to find appropriate diffusion values for the equipment design. The majority of those extensive diffusion studies is focused on the polymer films,[2–4] rather than the real polymer particles. The overall diffusion coefficients of internal diffusion in the pores of the polymer particles and diffusion in polymer matrix are those needed for the equipment design, and the diffusion coefficients in polymer films are not appropriate. Yan[5] determined the diffusion coefficients of dichloromethane, trichloromethane, tetrachloromethane, and n-hexane in polyethylene (PE) particles by use of the inverse gas chromatography, but the diffusion coefficients were infinite dilution ones. Gonzales[6] and Patzlaff[7] have reported the strong influence of the particle size on effective diffusion coefficients, but no quantitative relationship was obtained for lack of enough samples. Therefore, it is necessary to determine the diffusion behaviors of unreacted hydrocarbons in polyolefin particles quantitatively and comprehensively. It should also be mentioned that the concentration of hydrocarbons in polyolefin is always changing in the devolatilization process. The polyolefin after purging should contain hydrocarbons no more than 10 ppmw, which is a very dilute concentration. Hence, it is better to measure the effective diffusion coefficients and dilute diffusion coefficients simultaneously using a unified method.

The intelligent gravimetric analyzer (IGA) by Hiden Analytical (United Kingdom) is a weighing instrument with a high sensibility of 1 μg microbalance and an ultra-high vacuum. It can be well used to determine the diffusivity. Nobile et al.[8] validated a newly proposed model to predict the water-transport properties of multilayer polymer films, using the IGA apparatus. Limm

Table I. Characteristics of the Polyethylene Samples[a]

No.	Sample type	Density (g/cm^3)	MI (g/10 min)	M_w	M_w/M_n	T_m (K)	Crystallinity (DSC)	ε_p (%)
PE 1	LLDPE	0.918	2	96,458	3.9	394.25	0.272	34.09
PE 2	LLDPE	0.919	0.9	86,934	3.2	395.32	0.309	30.50
PE 3	HDPE	0.9456	12.2	163,364	16.2	401.32	0.544	30.01
PE 4	HDPE	0.9505	9	172,929	14.9	404.78	0.596	25.35
PE 5	HDPE	0.9508	2	225,776	15.9	406.52	0.615	21.55
PE 6	HDPE	0.9461	/	250,349	15.5	402.52	0.481	37.83
PE 7*	/	0.9312	0.03	527,231	4.1	408.89	0.378	71.02

[a]PE 7*: the sample was synthesized by our research group (polymerizations were conducted in a 1-L stainless steel continuous gas-phase-stirred bed reactor from Parr Instruments [Moline, IL] over a titanium-based Ziegler–Natta-type catalyst).

et al.[9] studied the diffusion coefficients of limonene in various linear low-density polyethylene (LLDPE) and low-density polyethylene resin films using the IGA gravimetric method. Doumenc[10] investigated the mutual diffusion coefficient of the polyisobutylene/toluene system through studying the swelling and the drying of polymer films by the IGA weighing methods. With its high sensibility of 1 μg, the IGA is appropriate to determine the dilute diffusion coefficients although no published study has been found.

In this study, the diffusion coefficients of 1-hexene, isopentane, and cyclohexane in PE particles were measured with the advanced microbalance—intelligent gravimetric analyzer, N_2 as the bypassing gas. Considering that ethylene and propylene diffuse much faster than 1-hexene, isopentane, and cyclohexane, the diffusion behavior of ethylene and propylene was not discussed in our study. The experiments were carried out under conditions relevant to solid-state devolatilization. The main aim is to study the effect of particle size, PE properties (crystallinity, density, and melt index [MI]), operating conditions (temperature and pressure) on the effective diffusion coefficients quantitatively. Moreover, the effective diffusion coefficients at dilute diffusant concentration were obtained, which are needed at the late stage of devolatilization.

EXPERIMENTS

Materials and Characteristics

Analytical grade isopentane (*i*-C_5H_{12}), 1-hexene (C_6H_{12}), and cyclohexane (C_6H_{14}) were obtained from J&K Chemical (Shanghai, China), with a minimum purity of 99.99%. The PE samples were supplied by SINOPEC (China) or synthesized by our research group. The samples were nascent particles obtained from the reactor after polymerization. The particles were mechanically sieved with meshes and the batch between mesh 20 and 30 (550–830 μm) was chosen for measurements.

The properties of PE samples are summarized in Table I. Density and MI were measured according to GB/T 1033-86 and GB/T 3682-83, separately. The molecular weight distribution and average molecular weight were obtained using the gel permeation chromatography (PL-220, United Kingdom). The differential scanning calorimetry (Perkin-Elmer 7, Japan) was used to determine the melting temperature and the crystallinity. For crystallinity determinations, a value of 290 J/g[11] was taken as the enthalpy of fusion of a perfectly crystalline material. The porosity (ε_p, defined as the ratio of the volume of pores in PE particle to the volume of the whole particle) was measured in the mercury intrusion porosimetry (MIP, IV-9510, USA).

The PE particles used for studying the influence of particle size were obtained by sieving the nascent particles of PE 1 into five different size fractions. The particle size and distribution are measured in the laser diffraction size analyzer (MASTERSIZER 2000, United Kingdom), taking the equivalent diameter of equal volume sphere as the mean particle diameter. The characteristics of the different size fractions are shown in Figure 1.

Apparatus and Measurements

The diffusion experiments were carried out in the IGA, model IGA-003, Hiden Analytical (Warrington, United Kingdom). A schematic diagram of the IGA is shown in Figure 2. The samples were placed in the reactor, which is a stainless steel cylinder with diameter of 34.5 mm and height of 300 mm. Temperature is regulated with a water bath or a heating furnace outside the reactor, and measured by a platinum resistance thermometer (Pt 100) located near the sample. The temperature uncertainty and stability are 0.1 and 0.05 K, respectively. Pressure is regulated with a proportional–integral–derivative (PID) controller, and measured by a manometer (relative error, <0.3%). The pressure stability is better than 2 Pa. At each set-pressure or

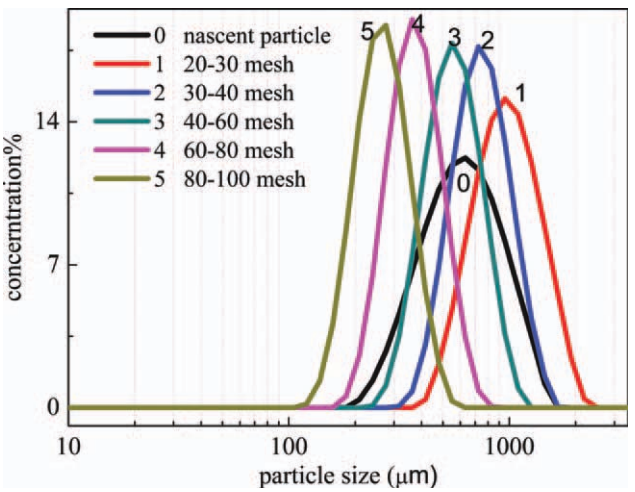

Figure 1. Particle size and distribution of fractions with different diameters. [Color figure can be viewed in the online issue, which is available at wileyonlinelibrary.com.]

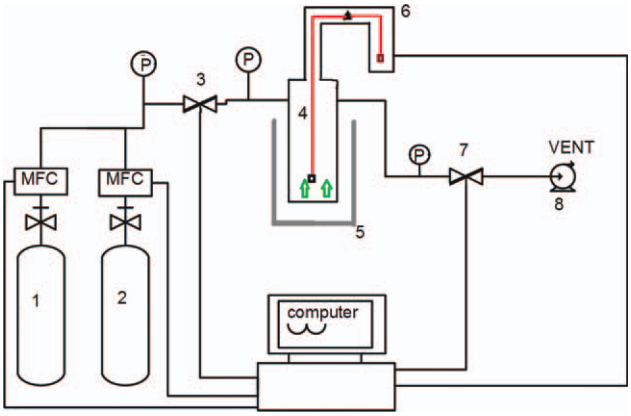

Figure 2. Schematic diagram of IGA-003 system: 1, 2: gas cylinder; 3: computer-controlled admittance valve; 4: reactor; 5: furnace; 6: computer-controlled thermostated microbalance system; 7: computer-controlled exhaust valve; 8: pump; MFC: mass flow controller; and P: pressure sensor. [Color figure can be viewed in the online issue, which is available at wileyonlinelibrary.com.]

temperature point, the real-time processor of the IGA can record the increase or decrease of the weight of the samples owing to adsorption or desorption of diffusant automatically. The mass measurement noise is about 1 μg, and the reproducibility (same measurement performed at various times) is about 10 μg.

Considering that the diffusion kinetics of sorption and desorption may differ, the desorption method was used and N_2 was the bypassing gas. The typical sample mass of the experiments is about 150 mg, not a constant, which would not influence the results. The PE particles were first outgassed in vacuum environment at 373 K for 24 h, to eliminate any existing unreacted hydrocarbons that might interfere with experiments. Second, the samples were immersed in the diffusant for 3 days, to make sure that they were saturated. Then, they were placed in the reactor. N_2 was introduced from the gas cylinder to purge the diffusant in particles. When the weight change was maintained at about 1 μg for more than half an hour, the diffusion equilibrium was assumed to be reached. The final procedure was to record the dry mass m_s of the PE.

Buoyancy and Swelling

Thermogravimetric analysis must be carefully corrected for a number of gravitational balance forces. In other words, buoyant forces have to be considered, including (1) changes in the buoyant forces owing to the variation in pressure and temperature; (2) aerodynamic drag force created by the flow of gases; (3) swelling (volumetric changes) in the samples owing to expansion. The sum of these forces is quite large (0.1–5 mg) and can lead to large errors if it is not carefully accounted for. The buoyancy correction follows from Archimede's principle. The true weight m is expressed as follows

$$m = m_{\text{meas}} + \rho_{\text{gas}}(p, T)V(p, T) \tag{1}$$

where m_{meas} is the apparent measured weight at pressure p and temperature T, ρ_{gas} (p, T) is the density of the gas phase, and $V(p, T)$ is the volume of the total measured object (comprising the volume of the polymer and accessories of the apparatus).

The temperature and pressure are usually not high in the devolatilization process of LLDPE and high-density PE technologies, and hence the solubilities of *i*-C_5H_{12}, C_6H_{12}, and C_6H_{14} are no more than 1 wt % separately. In the videomicroscopic measurements and PC-SAFT predictions by Novak,[12] no measurable swelling effect was observed for 1-hexene/PE particles system, under the conditions similar to our experiments. According to the relationship between elongation of PE film and solubility of 1-hexene in Moore's[13] study, the elongation is no more than 0.4% when the solubility is <1 wt %. Hence, swelling caused by adsorption of 1-hexene can be neglected in the buoyancy correction in our study. Owing to the lower or similar solubilities of *i*-C_5H_{12} and C_6H_{14}, no significant swelling of the PE particles is expected.

THEORY

Three kinds of mass-transfer patterns exist in PE particles: external mass transfer caused by particle packing, internal diffusion in the pores of the PE particles, and diffusion in PE matrix. The overall diffusion coefficients of internal diffusion and diffusion in polymer matrix are the needed ones. The overall diffusion can be expressed by Fick's second law,[7] assuming the particles are uniform spheres

$$\frac{\partial q}{\partial t} = D_{\text{eff}}\left(\frac{\partial^2 q}{\partial r^2} + \frac{2}{r}\frac{\partial q}{\partial r}\right) \tag{2}$$

Initial condition

$$q(r, 0) = q_0 \text{ at } t = 0$$

Boundary conditions

$$\frac{\partial q}{\partial r} = 0 \text{ at } r = 0$$

$$\frac{\partial q}{\partial r} = 0 \text{ at } r = R, \quad \text{that is } q|_{r=R} = \text{constant}$$

where D_{eff} is the effective diffusion coefficient of internal diffusion and diffusion in polymer matrix, and q is the concentration of diffusant in polymer particles, respectively.

The following assumptions are being made:

1. The adsorption equilibrium of N_2 in polymer particles is reached instantly, and keeps constant;
2. The swelling can be neglected as previous analysis;
3. The diffusion coefficient at low and dilute concentration is independent of concentration respectively; and
4. The flow rate of the bypassing gas is big enough to eliminate the external diffusion between particles.

Based on Crank's study,[14] solution of eq. (2) is

$$\frac{M_t}{M_\infty} = 1 - \sum_{n=1}^{\infty}\frac{6}{n^2\pi^2}\exp\left\{-D_{\text{eff}}n^2\pi^2 t/R^2\right\} \tag{3}$$

where M_t is the total amount of diffusant, leaving the sphere particles at time t, and M_∞ is the equilibrium value.

Effective diffusion coefficients can be determined by fitting the experimental desorption curves according to eq. (3).

RESULTS AND DISCUSSIONS

Determination of N_2 Flow Rate

As mentioned previously, three kinds of mass-transfer patterns exist in PE particles: external mass transfer caused by particle

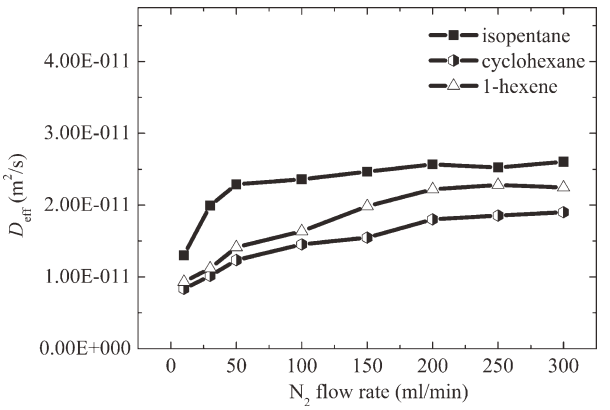

Figure 3. Diffusion coefficients of *i*-C_5H_{12}, C_6H_{14}, and C_6H_{12} in PE 1 under different N_2 flow rates.

packing, internal diffusion in the pores of the PE particles, and diffusion in PE matrix. Different particle packing results in different void fraction and external mass transfer. Besides, the overall diffusion of the internal diffusion and diffusion in PE matrix is what really needed to be investigated in the purging process. Hence, the flow rate of bypassing gas should be big enough to eliminate the external mass transfer. Desorption experiments of *i*-C_5H_{12}, C_6H_{12}, and C_6H_{14} in PE particles have been carried out under a series of N_2 flow rate, with the other conditions remained constant. The PE particles used here have the same average diameter, obtained by sieving PE 1 and the experiment temperature was 308 K. The pressure was constant in these experiments, and was maintained through a PID controller.

The results are shown in Figure 3. It can be seen that the effective diffusion coefficients of *i*-C_5H_{12}, C_6H_{12}, and C_6H_{14} vary little when the N_2 flow rate is >200 mL/min, which indicates that the influence of external mass-transfer resistance has been practically eliminated. To be on the safe side, the operation N_2 flow rate is determined as 300 mL/min.

Influence of PE Particle Size and Distribution

In this part, diffusion behaviors in PE 1 particles with different diameters have been investigated. The samples were obtained by sieving the nascent particles of PE 1 into five different size fractions. Different size fractions differ little in crystallinity,[5] and hence they are different only in particle size and distribution. *i*-C_5H_{12} diffuses faster than C_6H_{12} and C_6H_{14}, and hence we chose *i*-C_5H_{12} for these experiments to save time. The experiments were carried out at 308 K. The results of particle size and distribution have been shown in Figure 1. The diffusion results are shown in Figure 4. To ensure reproducibility, the experiments were repeated three times.

As shown in Figure 4, there is a significant dependency of the effective diffusion coefficients on particle size. Bigger particle size fraction results in bigger effective diffusion coefficient. For the fraction of the biggest particles, the effective diffusion coefficient is roughly one magnitude higher than that for the fraction of the smallest particles. The increase of effective diffusion coefficients with increasing polymer particle size is probably owing to the decrease of the effective length of diffusion within the polymer particle. This may be caused by the formation of more voids, cracks, or pores in the larger polymer particles during the course of polymerization.[7]

The second interesting but intriguing result in Figure 4 is that the effective diffusion coefficient is linear with the square of radius. Similar trends can be obtained from the effective diffusion coefficient values of ethylene in polypropylene copolymers and the corresponding radius in Bartke's study[15] although the author did not point it out.

It can also be observed that the red point representing diffusion result of nascent particles is right in the fitted line of sieved particles despite the nascent particles have larger size distribution. This can be explained by the following equation.

For the nascent particles, we can obtain the following equation via derivation

$$\frac{M_t}{M_\infty} = 1 - \sum_i X_i \sum_{n=1}^{\infty} \frac{6}{n^2\pi^2} \exp\left\{-D_{\text{eff},i} n^2 \pi^2 t / R_i^2\right\} \qquad (4)$$

where X_i, $D_{\text{eff},i}$, and R_i are mass fraction, effective diffusion coefficient, and mean radius of *i*th part of sieved particles, respectively. $D_{\text{eff},i}/R_i^2$ is a constant for the sieved particles; consequently $D_{\text{eff},i}/R_i^2$ is also a constant for the nascent particles.

The investigation above indicates that the effective diffusion coefficient is linear with the square of radius but has no obvious relationship with the particle size distribution. $D_{\text{eff},i}/R_i^2$ is taken as the parameter for comparison in the following studies.

Influence of PE Properties

In this part, the effect of PE properties (crystallinity, density, and MI) will be considered. The experiments were carried out at 308 K. Diffusion behaviors for semi-crystalline polymer films have been widely studied in terms of the noncrystalline fraction,[16,17] taking into account that the crystalline regions act as impermeable barriers. It is typically assumed that no solvent

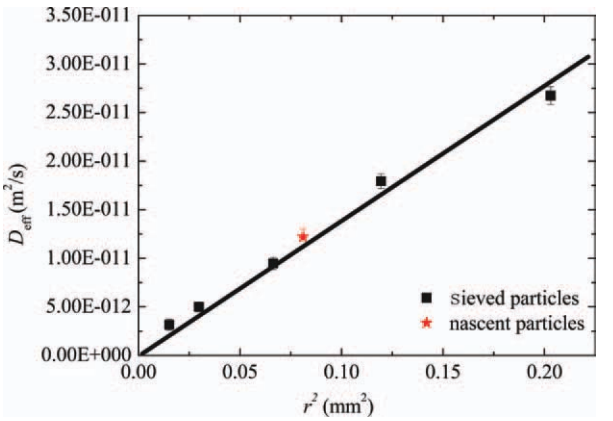

Figure 4. Dependency of effective diffusion coefficients on particle size for *i*-C_5H_{12} in PE 1. [Color figure can be viewed in the online issue, which is available at wileyonlinelibrary.com.]

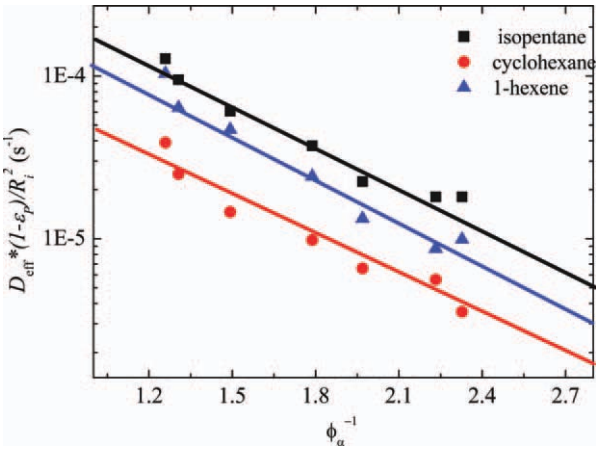

Figure 5. Semi-logarithmic plot of the normalized diffusion coefficients of various diffusants as a function of ϕ_α^{-1}. [Color figure can be viewed in the online issue, which is available at wileyonlinelibrary.com.]

can absorb into the crystalline regions of the polymer, and thus the solvent molecules must diffuse around them in a tortuous path. According to the reference published by Stern et al.,[18] the diffusion of small molecules through semi-crystalline polymers can be expressed in terms of Fujita's[19] free-volume model:

$$D = RTA_d \exp\left(-\frac{B_d}{\phi_\alpha v_f}\right) \tag{5}$$

where A_d and B_d are characteristic parameters; ϕ_α is the volume fraction of amorphous polymer, and can be determined from the crystallinity values (by DSC) reported in Table I. v_f is the volume fraction of the free volume; and R and T are the universal gas constant and absolute temperature, respectively. At low pressures as used in this study, v_f can be approximated by the following relationship:

$$v_f(T) = \frac{v_\alpha(T) - v_c(T)}{v_\alpha(T)} \tag{6}$$

where v_α (T) and v_c (T) are the specific volumes of the amorphous and crystalline phases, respectively. The temperature dependences of the specific volumes can be assumed to be[20]

$$v_\alpha(T) = 1.152 + 8.8 \times 10^{-4}(T - 273.15) \tag{7}$$

$$v_c(T) = 0.993 + 3.0 \times 10^{-4}(T - 273.15) \tag{8}$$

The PE particle samples are not only different in the form of crystallinity (Table I), but also in the form of pore properties (Table I). Hence, when we tried to build the relationship between effective diffusion and crystallinity, we considered only the matrix part. For the matrix part of a porous sphere

$$\frac{M_{t,\text{matrix}}}{M_{\infty,\text{matrix}}} = 1 - \sum_{n=1}^{\infty} \frac{6}{n^2\pi^2} \exp\{-(1-\varepsilon_p)D_{\text{eff}} n^2\pi^2 t/R^2\} \tag{9}$$

Then in the data analysis $(1 - \varepsilon_p)D_{\text{eff}}$ was used for correlation instead of D_{eff}. The terms A_d and B_d can be obtained from the least squares fit of the plot of $\ln[D_{\text{eff}}\ (1 - \varepsilon_p)/R_i^2]$ versus ϕ_α^{-1}

Table II. Values of the Free-Volume Parameters A_d and B_d

Diffusant	10^7 A_d(m²*mol/(s*J))	B_d
i-C_5	4.210	0.281
C_6H_{12}	3.700	0.310
C_6H_{14}	1.340	0.297

according to eqs. (5)–(9). The corresponding representation is shown in Figure 5, and a fairly good linear variation is observed.

The values obtained for A_d and B_d are listed in Table II. A_d depends on the diffusant molecular size. B_d is assumed to be a constant close to unity although more rigorous treatments suggest that its value depends on the size of the polymer jumping unit and the minimum size of the hole required for a diffusive jump to occur.[21]

The study above indicates that the effective diffusion coefficient normalized with radius and porosity has an exponential relationship with ϕ_α^{-1} at a certain temperature.

The density has a relationship with crystallinity as follows

$$w_c = \frac{\rho_c}{\rho}\left(\frac{\rho - \rho_\alpha}{\rho_c - \rho_\alpha}\right) \tag{10}$$

where $\rho_\alpha = 0.8531$ g/cm^3 and $\rho_c = 1.000$ g/cm^3 are the amorphous-phase and crystalline-phase densities, respectively, and ρ is the actual density of the polymer. The influence of density is given in eqs. (5)–(10).

The effect of MI was also considered. For PE 2, PE 3, and PE 4, they have similar normalized diffusion coefficients ($D_{\text{eff}}(1 - \varepsilon_p)/R_i^2 \approx 2.0 \times 10^{-5}$ s^{-1}) although they differ greatly in MI (Table I). While for PE 1 and PE 2, their normalized diffusion coefficients have difference as much as one magnitude (for PE 1, $D_{\text{eff}}(1 - \varepsilon_p)/R_i^2 = 1.3 \times 10^{-4}$ s^{-1}) although their MIs are equal (Table I). It can be seen that the MI has no distinct effect on the diffusion behavior.

Influence of Operating Conditions

The effect of operating conditions (temperature and pressure) on the diffusion behavior has also been analyzed. The PE

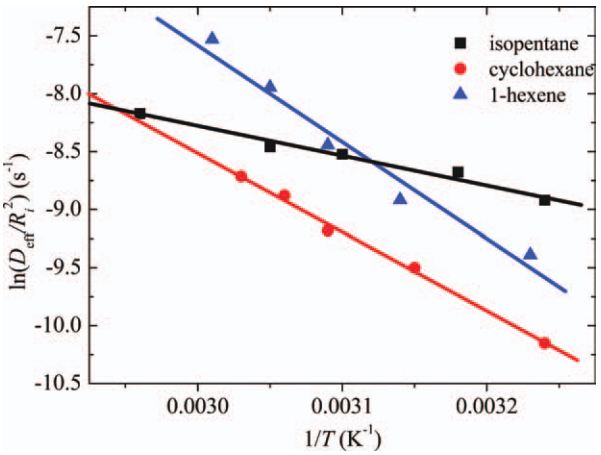

Figure 6. Variation of D_{eff}/R_{i2} with temperature for PE 1. [Color figure can be viewed in the online issue, which is available at wileyonlinelibrary.com.]

Table III. Arrhenius Coefficients of Various Diffusants in PE 1

Diffusant	D_0/R_i^2 (s^{-1})	E_{eff} (kJ/mol)
i-C_5H_{12}	0.450	20.750
C_6H_{12}	72470490	71.098
C_6H_{14}	160787.7	56.800

particles used here have the same average diameter, obtained by sieving PE 1.

The effect of temperature on the effective diffusion coefficients of *i*-C_5H_{12}, C_6H_{12}, and C_6H_{14} is shown in Figure 6. As expected, all the diffusion coefficients increase as the temperature increases. That is because the chains of PE become more flexible and the free volume in the PE matrix increases.[22] All effective diffusion coefficients are well correlated by an Arrhenius-type expression[23,24]:

$$D_{eff} = D_0 \exp\left(-\frac{E_{eff}}{RT}\right) \quad (11)$$

Here, D_0 is a temperature-independent pre-exponential factor, E_{eff} is the effective activation energy of diffusion, and RT has the usual conventional meaning. The Arrhenius coefficients were obtained through least square fitting and the results are summarized in Table III.

The variation of effective diffusion coefficient with the pressure was investigated. The operating pressure was achieved by adjusting the pressure of N_2 through a PID controller. The diffusant was *i*-C_5H_{12} and the PE sample was the sieved particle of PE 1. The effective diffusion coefficient almost maintains at the value of 2.50×10^{-12} m^2/s, in the range of 1–5 bar. Therefore, the effect of operating pressure could be neglected.

Diffusion at Dilute Concentration

The concentration of hydrocarbons in PE is always changing in the devolatilization process. Usually, the dependence of diffusant concentration on diffusion is not significant at low concentrations. For instance, diffusion coefficients of *i*-C_5H_{12} in nascent PE 1 particles at 308 K are roughly equal whether the initial *i*-C_5H_{12} concentration is 5000 or 1000 ppmw. However, the concentration of hydrocarbons at the late stage of devolatilization is very dilute because the PE should contain hydrocarbons no more than 10 ppmw after devolatilization for the purpose of safety and recycling. The dilute diffusion coefficient (defined as $D_{eff}^{\sim}$) can be one to two magnitudes lower than the effective one. Hence, it is not appropriate to consider D_{eff} being constant during the devolatilization stage.

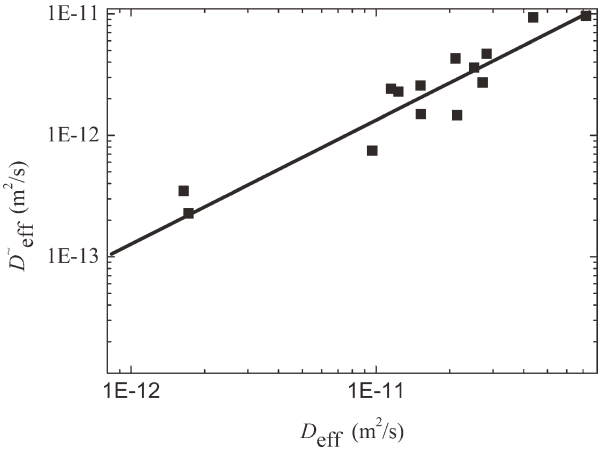

Figure 7. Log–log plot of the dilute diffusion coefficient versus the effective diffusion coefficient.

It is not necessary to consider D_{eff} as concentration dependent in the whole devolatilization stage. First, solving the diffusion equation needs efficient computer programs to obtain numerical or analytical solutions. Second, the application of complicate numerical or analytical solutions to practical problems can present difficulties, leading to calculation consumption in the design of devolatilization process, for example. Hence, we just adapted two effective diffusion coefficients for more simplicity and accuracy, D_{eff} at low concentrations and one at dilute concentrations (defined as $D_{eff}^{\sim}$).

Common balances for weighing are not accurate enough for obtaining $D_{eff}^{\sim}$. The IGA with a precision of 1 μg is appropriate for analyzing both the effective diffusion data and the dilute diffusion coefficient. $D_{eff}^{\sim}$ for most of the systems measured previously were acquired when the initial diffusant concentration was dilute, 100 ppmw. The relevant results are shown in Figure 7. $D_{eff}^{\sim}$ is about one magnitude smaller than D_{eff} and the logarithmic form of $D_{eff}^{\sim}$ is linear with that of D_{eff} through empirical fitting.

Table IV. The Comparison of Effective Diffusion Coefficients with the Literature Values

T (K)	System	Morphology	Thickness or diameter (mm)	Crystallinity	D_{eff} (m^2/s)	Literature	Method
298.15	C_6H_{14} + LLDPE	Particle	0.901	0.272	5.09e − 12	Our study	Desorption
298.15	C_6H_{14} + LDPE	Film	-[a]	-	3.34e − 12	Randová[25]	Swelling
333.15	*i*-C_5H_{12} + LLDPE	Particle	0.570	0.272	2.03e − 11	Our study	Desorption
333.15	*i*-C_5H_{12} + LLDPE	Particle	0.360	0.37	5-6e − 11	Scicolone[26]	IGC[b]
343.15	C_6H_{12} + LLDPE	Particle	0.901	0.272	2.21e − 10	Our study	Desorption
343.15	C_6H_{12} + LLDPE	Particle	0.360	0.37	1.35e − 10	Scicolone[26]	IGC

[a]Not found in relevant literatures. [b]Not found in relevant literatures.

Comparison with the Literature Values

Effective diffusion coefficients calculated from the crystallinity dependence (eq. 5) and temperature dependence (eq. 11), using the parameters listed in Tables II and III, are compared with the data found in the literatures. The results are summarized in Table IV. It can be seen that diffusion coefficients are of the same order as the literature values. The difference may be caused by different apparatus, methods, or PE shapes.

CONCLUSIONS

A desorption method by the IGA was developed to measure effective diffusion in polymer particles–solvent systems. Both the effective diffusion data and the dilute diffusion coefficient can be obtained. The results showed that $D_{\text{eff}}^{\sim}$ was about one magnitude smaller than D_{eff} and the logarithmic form of $D_{\text{eff}}^{\sim}$ was linear with that of D_{eff}. Besides, the effects of particle size, PE properties, and operation conditions on D_{eff} were investigated. It was found that D_{eff} was linear with the square of the particles' average radius. The influence of PE crystallinity was indicated by the relationship of normalized diffusion coefficients with ϕ_{α}^{-1}, according to Fujita's free-volume theory. The dependence of D_{eff} for all systems on temperature was correlated well with the Arrhenius equation. The particle size distribution, MI, and operating pressure showed no obvious effect on D_{eff}.

In this article, the effective diffusion coefficient values are not only necessary in the design of devolatilization, no matter in the gas or slurry technology, but also of profound importance for studying the process of polymerization in reactors, granulation, and drying.

ACKNOWLEDGMENTS

The authors gratefully acknowledge financial support from National Natural Science Foundation of China (21176208).

REFERENCES

1. Tadmor, Z.; Gogos, C. G. Principles of Polymer Processing, 2nd ed.; John-Wiley & Sons: New York, **2006.**
2. Kiparissides, C.; Dimos, V.; Boultouka, T.; Anastasiadis, A.; Chasiotis, A. *J. Appl. Polym. Sci.* **2003,** *87*, 953.
3. Beret, S.; Hager, S. L. *J. Appl. Polym. Sci.* **1979,** *24*, 1787.
4. Castro, E. F.; Gonzo, E. E.; Gottifredi, J. C. *J. Membr. Sci.* **1987,** *31*, 235.
5. Yan, X. W.; Shan, Y. B.; Wang, J. D.; Yang, Y. R. *J. Chem. Ind. Eng. (China)* **2007,** *8*, 1917.
6. Gonzales, A.; Eceolaza, S.; Etxeberria, A.; Iruin, J. J. *J. Appl. Polym. Sci.* **2007,** *104*, 3871.
7. Patzlaff, M.; Wittebrock, A.; Reichert, K. H. *Macromol. Symp.* **2006,** *236*, 235.
8. Del Nobile, M. A.; Buonocore, G. G.; Dainelli, D.; Nicolais, L. J. *Food Sci.* **2004,** *69*, 85.
9. Limm, W.; Begley, T. H.; Lickly, T.; Hentges, S. G. *Food Addit. Contam.* **2006,** *23*, 738.
10. Doumenc, F.; Guerrier, B.; Allain, C. *Polymer* **2005,** *46*, 3708.
11. Flory, P. J.; Vrij, A. J. *J. Am. Chem. Soc.* **1961,** *85*, 3548.
12. Novak, A.; Bobak, M.; Kosek, J.; Banaszak, B. J.; Lo, D.; Widya, T.; Harmon Ray, W.; de Pablo, J. J. *J. Appl. Polym. Sci.* **2006,** *100*, 1124.
13. Moore, S. J.; Wanke, S. E. *Chem. Eng. Sci.* **2001,** *56*, 4124.
14. Crank, J. The Mathematics of Diffusion; Clarendon Press: Oxford, **1975.**
15. Bartke, M.; Kröner, S.; Wittebrock, A.; Reichert, K. H.; Illiopoulus, I.; Dittrich, C. J. *Macromol. Symp.* **2007,** *259*, 327.
16. Michaels, A. S.; Bixler, H. J. *Chem. Phys.* **1961,** *50*, 393.
17. Laguna, M. F.; Cerrada, M. L.; Benavente, R.; Perez, E.; Quijada R. *J. Polym. Sci. B Polym. Phys.* **2003,** *41*, 2174.
18. Stern, S. A.; Sampat, S. R.; Kulkarni, S. S. *J. Polym. Sci. B Polym. Phys.* **1986,** *24*, 2149.
19. Fujita, H. *Adv. Polym. Sci.* **1961,** *3*, 1.
20. Chiang, R.; Flory, P. J. *J. Am. Chem. Soc.* **1963,** *85*, 2857.
21. Compañ, V.; Andrio, A.; López, M. L.; Riande, E. *Polymer* **1996,** *37*, 5831.
22. Joseph, A.; Mathai, A. E.; Thomas, S. *J. Membr. Sci.* **2003,** *220*, 13.
23. Pickup, S.; Blum, F. D. *Macromolecules* **1989,** *22*, 3961.
24. Nystrom, B.; Moseley, M. E.; Brown, W.; Roots, J. *J. Appl. Polym. Sci.* **1981,** *26*, 3385.
25. Randová, A.; Bartovská, L.; Hovorka, Š.; Bartovsky, T.; lzák, P.; Poloncarzová, M.; Friess, K. *e-Polymers* **2010,** *068*, 1.
26. Scicolone, J. V.; Davis, P. K.; Danner, R. P.; Duda, J. L. *Polymer* **2006,** *47*, 5364.